

## Recurrence spectroscopy of atoms in electric fields: Failure of classical scaling laws near bifurcations

John A. Shaw and F. Robicheaux

*Department of Physics, Auburn University, Auburn, Alabama 36830*

(Received 23 May 1997)

The photoabsorption spectra of atoms in a static external electric field shows modulations from *recurrences*: electron waves that go out from and return to the vicinity of the atomic core. Closed-orbit theory predicts the amplitudes and phases of these modulations in terms of closed classical orbits. A classical scaling law relates the properties of a closed orbit at one energy and field strength to its properties at another energy and field strength at fixed scaled energy  $\epsilon = EF^{-1/2}$ . The scaling law states that the recurrence strength of orbits along the electric field axis scale as  $F^{1/4}$ . We show how this law fails near bifurcations when the effective Planck constant  $\hbar \equiv \hbar F^{1/4}$  increases with increasing field at fixed  $\epsilon$ . The recurrences of orbits away from the axis scale as  $F^{1/8}$  in accordance with the classical prediction. These deviations from the classical scaling law are important in interpreting the recurrence spectra of atoms in current experiments. This leads to an extension of the uniform approximation developed by Gao and Delos [Phys. Rev. A **56**, 356 (1997)] to complex momenta. [S1050-2947(98)10309-8]

PACS number(s): 32.60.+i, 03.65.Sq

### I. INTRODUCTION

Experiments show oscillations in the average photoabsorption rate from low-lying initial states to unresolved final states near the ionization threshold of atoms in external electric and magnetic fields [1–3]. Closed-orbit theory attributes these oscillations to classical orbits of the electron that begin and end near the nucleus [4,5]. The wavelengths of the oscillations on the energy axis are related to the closure times  $T$  of the classical orbits by  $\lambda_E = h/T$  and the amplitude of each oscillation is inversely proportional to the divergence rate of the neighbors for each orbit. Therefore, a Fourier transform of an experimental or a calculated quantum photoabsorption spectrum gives information about the closed classical orbits in the system. The absolute square of the Fourier transform of such an absorption spectrum is the “recurrence spectrum.” It has peaks at the closure times of the closed orbits and the height of each peak is the “recurrence strength” for that orbit.

In this paper we compare quantum and semiclassical calculations for hydrogen at fixed scaled energy in an electric field for different ranges of  $E$  and  $F$  (we use  $F$  for the electric field strength to avoid confusion with the energy  $E$ ). Results for  $m=0$  and 1 spectra are reported. Quantum calculations and semiclassical calculations for  $\epsilon = -3.0$  have been published for H and Li [3,6]. Experiments for He have been performed by Keeler and Morgan and are being planned by Kips and Hogervorst [7].

The recurrence spectrum is best studied in scaled-variable experiments, in which the photon energy and the external fields are varied simultaneously to keep the scaled energy fixed, in an electric field  $\epsilon = EF^{-1/2}$ . Associated with  $\epsilon$  is a scaled classical Hamiltonian  $\hat{H} = HF^{-1/2}$ . Although classical mechanics is invariant under this scale change, quantum mechanics has a natural scale set by  $\hbar$ . The size of the scaled coordinates and momenta relative to  $\hbar$  vary with the field strength  $F$ . The ratio of the action along an orbit to  $\hbar$ ,  $S/\hbar$ ,

in particular becomes  $\hat{S}(\epsilon)2\pi F^{-1/4}$  in scaled variables and this quantity determines the phase of the returning semiclassical waves. The “effective Planck constant” is defined as  $\hbar = F^{1/4}$  in atomic units. Thus  $\hbar$  can be changed at fixed  $\epsilon$  simply by varying the electric field range measured in the experiment. Smaller  $F$  at fixed  $\epsilon$  implies higher principal quantum numbers  $n$ , while larger  $F$  implies lower. We show an example recurrence spectrum where the primitive semiclassical approximation that gives good agreement with quantum calculations and experiment in the small- $\hbar$ , high- $n$  regime must be replaced by a uniform semiclassical approximation as the field strength is increased even though the classical mechanics of the system has been kept fixed. The uniform approximation takes into account that related orbits with having actions within  $\hbar$  of each other cannot be considered in isolation.

An overview of uniform approximations in closed orbit theory has been written recently by Main and Wunner [8] and uniform approximations have been applied to periodic-orbit theory by Schomerus and Sieber [9]. Many earlier works exist on uniform approximations and catastrophe theory [10–12].

The semiclassical recurrence strength of an isolated closed-orbit in hydrogen at a fixed value of  $\epsilon$  scales as  $(F/F_o)^{1/8}$  except for the orbits that are on the  $\pm z$  axes, which scale as  $(F/F_o)^{1/4}$ . Here  $F_o$  is fixed and once the classical orbits and recurrence strengths are computed at this field strength, the recurrence strength is known along the entire line satisfying the constraint  $\epsilon = EF^{-1/2}$ . Both formulas predict an increase in the recurrence strength as the field strength is increased. The recurrence strength of the on-axis orbit is predicted to grow faster than the recurrence strength of other orbits as  $F$  increases.

When  $F$  increases sufficiently at fixed  $\epsilon$ , these semiclassical scaling laws will begin to fail because of the increased size of  $\hbar$ , but there has been little work that quantifies this

nonscaling, especially in a system amenable to experiment. Atoms in electric fields are simple systems in which to study these effects. First, we show that the  $m=1$  spectra follow the scaling law while the  $m=0$  spectra do not. Second, in the  $m=0$  spectra the first recurrence strengths that deviate from the scaling law are the recurrences due to orbits near the  $\pm z$  axes. The recurrence strengths of these orbits in our quantum calculation can decrease relatively to the recurrences of the other orbits in the system, in contradiction to the classical scaling prediction. Third, we show that this comes from the breakdown of the isolated orbit approximation. As  $\hbar$  increases, orbits near the  $\pm z$  axis that are isolated at low electric field strengths are no longer isolated at higher field strengths. The recurrences from these orbits can be calculated semiclassically with a uniform approximation developed by Gao and Delos. Their method works when the closed orbits involved are real, but Gao and Delos did not develop a method of including the complex orbit contributions before the bifurcation. We have a simple method of locating the complex orbits and calculating the uniform recurrence strength when both real and complex orbits contribute. Therefore, we can easily study the changes in recurrence spectra from complex orbits as well as real orbits as functions of scaled energy and the size of  $\hbar$  and use this to understand the failure of the classical scaling law. There is a simple formula for the field strength where the uniform approximation becomes necessary for a given scaled energy.

## II. CLOSED-ORBIT THEORY

### A. Recurrence integrals

Closed-orbit theory divides the configuration space into an inner and outer region. In the inner region we have the Coulomb problem with a mixture of regular and irregular Coulomb functions determined by the quantum defects of the ionic core. In the outer region we have the Coulomb attraction plus the external field and we can use a semiclassical approximation to the Green's function  $G_E^+$ . The average oscillator strength density for a transition is proportional to the imaginary part of the overlap matrix

$$\overline{Df} = -2\pi^{-1}(E - E_i)\text{Im}\langle D\psi_i | G_E^+ | D\psi_i \rangle, \quad (1)$$

where  $\psi_i$  is the initial state,  $D$  is the relevant component of the dipole operator of the laser, and  $G_E^+$  is the outgoing Green's function for electrons of energy  $E$ . In this formula,  $|D\psi_i\rangle$  effectively constitutes a ‘‘source’’ and  $G_E^+ |D\psi_i\rangle$  are waves that go out at constant energy from this source. Those waves that later return to the source contribute to the integral  $\langle D\psi_i | G_E^+ | D\psi_i \rangle$ , which governs the absorption rate. A ‘‘primitive’’ semiclassical approximation to the Green's function gives a sum of returning waves associated with each distinct closed classical path.

Each such return constitutes a classical recurrence. These are labeled by two indices  $(k, n)$  where  $k$  labels the particular closed orbit and  $n$  is the number of returns to the origin. If we ignore core scattering, then the returning waves associated with a closed orbit  $\Lambda_{return}^{k,n}(\vec{q})$  are simply turned around by the Coulomb field and they go back out in the direction

from which they came, later to return to give the  $(k, n+1)$  recurrence.

It is useful to define the ‘‘ $(k, n)$  recurrence integral’’

$$R_k^n \equiv \langle D\phi_i | \Lambda_{return}^{k,n} \rangle. \quad (2)$$

Then the oscillator strength is approximated by

$$\overline{Df} = -2\pi^{-1}(E - E_i)\text{Im}\sum_{k,n} R_k^n. \quad (3)$$

Formulas for these recurrence integrals were developed in [4,13]. One finds

$$R_k^n = 2^{3/2}\pi\mathcal{Y}(\theta_f^{k,n})N_k^n, \quad (4)$$

where  $\mathcal{Y}(\theta)$  is the angular distribution of the initial outgoing wave [13].

The quantity  $N_k^n$  contains information about the amplitude and phase of the returning wave coming from a particular direction. For the orbits parallel or antiparallel to the field direction (‘‘uphill’’ and ‘‘downhill,’’ labeled  $k=0$  or  $\pi$ , respectively) it is

$$N_0^n = 4\pi i r_o^{-1/2} \left| \frac{\partial \theta_f^{0,n}}{\partial \theta_i} \right|^{-1} \exp \left[ i \left( S_0^n / \hbar - \mu_0^n \frac{\pi}{2} \right) \right] \mathcal{Y}(0), \quad (5)$$

while for all other orbits it is

$$N_k^n = -2^{9/4}\pi^{3/2}e^{-i3\pi/4}r_o^{-1/4}|\sin\theta_i^k \sin\theta_f^{k,n}|^{1/2} \times \left| \frac{\partial \theta_f^{k,n}}{\partial \theta_i} \right|^{-1/2} \exp \left[ i \left( S_k^n / \hbar - \mu_k^n \frac{\pi}{2} \right) \right] \mathcal{Y}(\theta_i^k). \quad (6)$$

Here  $\theta_i$  and  $\theta_f$  are initial and final angles,  $S$  is the action all the way around the orbit,  $\mu$  is the Maslov index for the returning wave, and  $r_o$  is a boundary on which  $\partial \theta_f / \partial \theta_i$  is evaluated; each is labeled as needed for the  $n$ th return of the  $k$ th closed orbit.

Now  $N_0^n$  and  $N_k^n$  are matching constants derived by doing a stationary phase integral about the direction of the incoming electron  $\theta_f^{k,n}$  [4] and two approximations were used in deriving Eqs. (5) and (6). In the first, the returning wave can be described as an azimuthally rotated zero-energy Coulomb wave coming in from the direction  $\theta_f^{k,n}$ . In the second, the closed orbit is isolated from its neighbors. This is equivalent to the assumption that only one stationary phase point contributes to the integral. This second condition is violated near the bifurcations of a closed orbit where multiple stationary phase points merge. Since only stable orbits can bifurcate into new orbits or, in the inverse bifurcation, absorb orbits and destroy them [8,14], only the uphill and downhill orbits in this system can bifurcate and all bifurcations occur near the  $\pm z$  axes.

When is a stationary phase point isolated? If we consider integrals of the form

$$K = \int_{-\infty}^{\infty} A(q) \exp \frac{i}{\hbar} S(q) dq, \quad (7)$$

then the dominant contribution comes from the vicinity of points  $q_n$ , where  $\partial S / \partial q = 0$ . The point  $q_0$  is isolated from

another stationary phase point, call it  $q_1$ , if the ratio of  $|S(q_1) - S(q_0)|$  to  $\hbar$  is large [15].

$S/\hbar$  in Eqs.(5) and (6) becomes  $\hat{S}(\epsilon)2\pi F^{-1/4}$  in scaled variables, so for fixed scaled energy the approximations used to derive Eqs. (5) and (6) will fail as  $\hbar$  increases if the stationary phase points in the bifurcation satisfy the inequality

$$2\pi|\hat{S}_k^{n'} - \hat{S}_k^n| \leq F^{1/4} = \hat{\hbar}. \quad (8)$$

The coalescence of stationary phase points is treated properly by going to a uniform approximation.

### B. Uniform recurrence integrals

A uniform approximation for the hydrogen atom in the electric field was developed by Gao and Delos [16,17]. We have implemented this method and have extended it to include scattering off an alkali-metal core. Let us outline the theory and give the results for the uniform recurrence integral.

For an electric field along the  $z$  axis in spherical coordinates we use scaled semiparabolic coordinates  $(u, v, p_u, p_v, \tau)$  [13,18,19] defined by

$$\begin{aligned} \hat{r} &= \frac{1}{2}(u^2 + v^2), & \hat{r} &= rF^{1/2}, \\ \hat{z} &= \frac{1}{2}(u^2 - v^2), & \hat{z} &= zF^{1/2}, \\ \frac{d\hat{t}}{d\tau} &= u^2 + v^2, & \hat{t} &= tF^{3/4}. \end{aligned} \quad (9)$$

The Hamiltonian in scaled semiparabolic coordinates is

$$\begin{aligned} \hat{H} &= \frac{1}{2}(p_u^2 + p_v^2) + \frac{m^2}{2u^2} + \frac{m^2}{2v^2}, \\ &- \epsilon(u^2 + v^2) + \frac{1}{2}(u^4 - v^4) = 2, \end{aligned} \quad (10)$$

where  $m$  is the  $z$  component of the angular momentum,  $\epsilon$  is the scaled energy, and  $p_u$  and  $p_v$  are  $du/d\tau$  and  $dv/d\tau$ , respectively. There is a complication: The orthogonal coordinates  $u$  and  $v$  correspond to the  $z$  and  $-z$  axes in real space and therefore are both axes of cylindrical symmetry. As a result, the uniform approximation will involve a Fresnel integral instead of a Pearcey integral [17,20].

Hamilton's equations of motion are used to calculate the closed orbits in  $(u, v)$  space. The  $(u, v)$  transformation removes the Coulomb singularity. Since the uniform approximation is needed only for the uphill and downhill orbits, which do not exist for  $m=1$ , we set  $m=0$  in this section and start the trajectories from the origin  $u=v=0$ . The initial direction is given by  $\Theta_i = \tan^{-1}(p_{v_i}/p_{u_i})$ , with  $0 \leq p_{v_i} \leq 2$  and  $p_{u_i} = \sqrt{4 - p_{v_i}^2}$ . This angle is half the angle  $\theta$  in spherical coordinates. The trajectories evolve in the potential and then return towards the origin. We define a Poincaré surface of section  $(p_v, v)$  with  $u=0$  and record  $p_{v_f}$  and  $v_f$  when the trajectory crosses the surface in either direction. This works for  $0 \leq \Theta_i < \pi/2$ . For the downhill orbit,  $\Theta_i = \pi/2$ , the

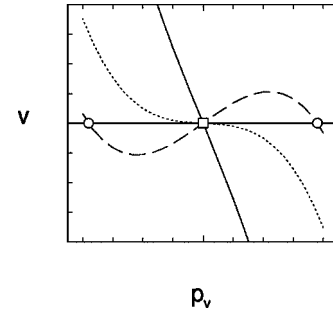


FIG. 1. Calculated Lagrangian manifolds before (solid line), near (dotted line), and after (dashed line) a bifurcation of the uphill orbit is shown. The uphill orbit (square symbol) exists for each scaled energy while the newly bifurcated orbits (circles) only exist after the bifurcation.

$(p_v, v)$  surface of section is inappropriate, and we define a surface of section  $(p_u, u)$  with  $v=0$  and a manifold on that surface. The following discussion holds for the downhill orbit if we replace  $(p_v, v)$  by  $(p_u, u)$  everywhere.

A plot of  $v_f$  vs  $p_{v_f}$  on the surface of section traces out the Lagrangian manifold. The Lagrangian manifold intersects the  $p_v$  axis at points  $p_{v_f}$  whenever  $v_f=v=0$  and these are the locations of the closed orbits. The semiclassical amplitude of the returning wave associated with the closed orbit is related to the inverse of the slope  $\partial v_f / \partial p_{v_f}$  of the manifold at these points. This derivative can be related to  $\partial \theta_f^{k,n} / \partial \theta_i$  in Eq. (5) [18].

The shape of the Lagrangian manifold determines the type of bifurcation. In this system orbits are created from the uphill orbit and destroyed by the downhill orbit in cusp bifurcations modified by the cylindrical symmetry about the  $\pm z$  axes. Near a cusp bifurcation on the  $z$  axis, the manifold is nearly cubic about  $p_v=0$ . On one side of the bifurcation the manifold will intersect the  $p_v$  axis at only one point  $p_{v_f}=0$ , corresponding to one real closed orbit. The other roots of the cubic manifold are complex, corresponding to imaginary orbits with complex momenta. At the bifurcation the slope of the manifold is zero. After the bifurcation, two new intersections with the  $p_v$  axis at  $\pm p'_v$  move away from  $p_{v_f}=0$ . The manifold now has three real closed orbits with momenta  $p_{v_f}=0, \pm p'_v$ . This is shown in Fig. 1. At the bifurcation energy the semiclassical amplitude predicted by Eq. (5) is infinite. Near the bifurcation energy, inserting Eq. (5) into Eq. (4) will greatly overestimate the recurrence strength.

The semiclassical representation of the coordinate space wave function is constructed by the projection of the manifold onto the  $(u, v)$  coordinate axes [21]. At the bifurcation the  $v$  projection fails, but the projection of the manifold onto the mixed  $(u, p_v)$  coordinate and momentum space axes is well behaved. If we go into the mixed space representation of the wave function when we are near a bifurcation and transform this mixed space representation back into the coordinate space, then we get a well behaved, finite, coordinate space wave function.

Gao and Delos show that the uniform coordinate space wave function near the bifurcation of the uphill orbit is given by

$$\Lambda_{\text{unif}}^{0,n} = D' \int_{p_v} A(p_v) \exp[iF(p_v)] \mathcal{Y}(2\Theta_i) \times J_0(p_v v / \hbar) J_0(p_u u / \hbar) p_v dp_v, \quad (11)$$

where

$$A(p_v) = \left| \frac{p_{v_i}}{p_{v_f}} \frac{\partial p_{v_i}}{\partial p_{v_f}} \right|^{1/2}, \quad (12)$$

$$F(p_v) = \left\{ \tilde{S}_0^n(\epsilon) - \frac{a_1(\epsilon)}{2} p_v^2 - \frac{a_3(\epsilon)}{4} p_v^4 \right\} / \hbar - \nu \frac{\pi}{2}, \quad (13)$$

and  $D' = -\pi 2^{3/2}$  is a constant. The function  $F(p_v)$  is the mixed-space action, the generator of the Lagrangian manifold, evaluated on the  $n$ th intersection of the surface of section  $u=0$ . Since  $p_{v_f} = -\partial F(p_v) / \partial p_v$  this reproduces the cubic manifold and the closed orbits are located at the roots,  $p_{v_f} = 0, \pm \sqrt{-a_1/a_3}$ . The mixed space action can be directly calculated from the formula

$$\tilde{S}(p_v, u) = \int p_u du - \int v dp_v \quad (14)$$

and fitted to Eq. (13) on the surface of section to get  $a_1$  and  $a_3$ . The mixed-space actions  $\tilde{S}$  and the scaled coordinate space actions  $2\pi\hat{S}$  coincide at the closed orbits. The uniform recurrence integral is given by

$$R_0^{\text{unif},n} = \langle D \phi_i | \Lambda_{\text{unif}}^{0,n} \rangle = D' 2^{3/2} \pi \int_{p_v} A(p_v) \exp[iF(p_v)] \times \mathcal{Y}(2\Theta_i) \tilde{\mathcal{Y}}(2\Theta_f) p_v dp_v. \quad (15)$$

### C. Evaluating the recurrence integral

The uniform recurrence integral eliminates the divergence in the primitive semiclassical approximation. The evaluation of this integral when two of the stationary phase points  $\pm p_{v_f}$  are complex and the field strength dependence of Eq. (15) must now be examined.

The integral in Eq. (15) is converted to a Fresnel integral in the variable  $x \equiv p_v^2$  with an additional end-point correction from  $x=0$ . The closed orbits correspond to the roots of the cubic manifold at  $p_{v_f}=0$  and  $\pm \sqrt{-a_1/a_3}$ . Complex momenta must be considered when  $a_1/a_3$  is positive and only the on-axis orbit with  $p_{v_f}=0$  is real.

If we define

$$g(p_v) = \mathcal{Y}(\theta_i) \tilde{\mathcal{Y}}(\theta_f) \left| \frac{p_{v_i}}{p_{v_f}} \frac{\partial p_{v_i}}{\partial p_{v_f}} \right|^{1/2} \quad (16)$$

and change variables to  $x$ , then

$$R_0^{\text{unif},n} = D'' \int_{x=0} g(x) \exp\{i\lambda(\frac{1}{2}x^2 + ax)\} dx, \quad (17)$$

where  $a = a_1/a_3$ ,  $\lambda = -a_3/2\hbar$ , and  $D'' \equiv -\pi^2 2^3 \exp\{i(\hat{S}_0/\hbar - \nu\pi/2)\}$  is a complex constant. Eq. (17) has stationary phase points at  $x = -a$  and 0.

The amplitude  $g(x)$  can be expanded in a power series about  $x=0$ , the location of the on-axis orbit,

$$g(x) = g_0 + g_1 x + g_2 x^2. \quad (18)$$

The bifurcations occur when  $a(\epsilon)$  passes through zero,  $\epsilon = \epsilon_{\text{bif}}$ . If  $a$  is negative, then real roots and real closed orbits exist that begin and end with momenta  $p_v = \pm \sqrt{a}$ . If  $a$  is positive, then imaginary roots and complex closed orbits exist that begin and end with momenta  $p_v = \pm i\sqrt{a}$ . However,  $x$  is still real, even though the momenta of the orbits have become imaginary, and we can use  $x = -a$  in Eq. (18) to calculate the amplitude at the complex stationary phase points of Eq. (17).

We can now get the analytic form of the recurrence integral in the neighborhood of  $\epsilon = \epsilon_{\text{bif}}$ . We substitute Eq. (18) into Eq. (17), change integration variables to  $u = x + a$ , and collect terms with the same power of  $u$  under the integral. The result is

$$R_0^{\text{unif},n} = D'' \left\{ g(a) e^{-i(\lambda/2)a^2} D(\lambda; a) + \frac{i}{\lambda} \frac{\partial g}{\partial x} \Big|_{x=-a} + O(u^2) \right\}, \quad (19)$$

where

$$g(a) = g_0 - g_1 a + g_2 a^2, \quad (20)$$

$$\frac{\partial g}{\partial x} \Big|_{x=-a} = g_1 - 2a g_2, \quad (21)$$

and

$$D(\lambda; a) = \int_a^\infty e^{i(\lambda/2)x^2} dx = \frac{1}{2} \sqrt{\frac{\pi}{\lambda}} [1 + \text{sgn}(\lambda) i] - \sqrt{\frac{\pi}{\lambda}} \left\{ C \left( \sqrt{\frac{\pi}{\lambda}} a \right) + \text{sgn}(\lambda) i S \left( \sqrt{\frac{\pi}{\lambda}} a \right) \right\}. \quad (22)$$

The  $C$  and  $S$  in Eq.(22) are standard Fresnel integrals [22,23] and  $\text{sgn}(\lambda)$  is the sign of  $\lambda$ . The field strength dependence of Eq. (22) is in the parameter  $\lambda$ , which is proportional to  $F^{-1/4}$ , i.e.,  $1/\hbar$ . The parameter  $a$  depends only on  $\epsilon$ .

The coefficients  $g_0$ ,  $g_1$ , and  $g_2$  can be calculated when the mixed-space action is calculated by integrating trajectories for a range of  $p_{v_i}$  until they reach the surface of section  $(p_v, v)$  for  $u=0$ . The functions  $g(p_v)$  and  $\tilde{S}(p_v)$  are then known from Eqs. (16) and (14) and  $g(p_v)$  and  $\tilde{S}(p_v)$  are fitted to polynomials in  $p_v^2$  and  $p_v^4$ . In principle, the calculated manifold should be transformed by an addition change of variables to normal form, but the deviation of the Lagrangian manifold from a cubic polynomial is very small for the bifurcations of the uphill orbit in the scaled-energy range below  $\epsilon = -2$  so the root positions can be calculated directly from the fitted manifold. The Lagrangian manifold near the downhill orbit is more strongly curved and the deviation

from the cubic form can be significant for bifurcations near  $\epsilon = -2$ . Between  $\epsilon = -2.1$  and  $-3.0$  the cubic approximation for the downhill orbit manifold becomes very good.

Equation (19) should be compared to the uniform result of Bleistein [24]. The Bleistein formula as adapted by Gao [16] is

$$R_0^{\text{unif},n} = D'' \left\{ g(a) e^{-i(\lambda/2)a^2} D(\lambda; a) + \frac{g(a) - g(0)}{a} \frac{i}{\lambda} \right\}, \quad (23)$$

where  $g(0)$  is the amplitude of the uphill orbit,  $\theta_i = 0$ , and  $g(a)$  is the amplitude of the new closed orbit. This was the formula used to calculate the spectra in [16,17] when the momenta were real. Near the bifurcation the finite difference term  $[g(a) - g(0)]/a$  in Eq. (23) was taken to be a constant, equal to the limiting value as  $a(\epsilon) \rightarrow 0$  from below [16]. When  $a$  was large and positive the asymptotic form of the terms involving  $g(a)$  was shown to cancel so only  $g(0)$  remained, giving the isolated orbit result [16]. However, the behavior between the bifurcation energy and the isolated orbit result could only be estimated by extrapolation from  $\epsilon = \epsilon_{\text{bif}}$  and approximations. This leads to problems since the approximations appropriate near the bifurcation do not give the correct asymptotic behavior needed to get the isolated orbit result away from the bifurcation. Since Eqs. (19) and (23) are equivalent near the bifurcation,  $g(a)$  and  $[g(a) - g(0)]/a$  can now be calculated with Eq. (20) when the momenta are complex. By inserting the proper complex stationary phase points into Eq. (23) we get results that are smooth functions of  $\epsilon$  and  $\hbar$ . In particular, the Bleistein formula now smoothly goes to the isolated on-axis orbit recurrence strength in the limit  $a(\epsilon) \rightarrow +\infty$  as  $\epsilon$  is varied at fixed field strength if we use Eq. (20) to calculate the contributions of the complex momenta. No extrapolation is needed. It is the  $\epsilon$  and  $\hbar$  dependence of the Bleistein formula with real and complex contributions that determines the scaling or nonscaling of the recurrence spectra measured in experiments.

### III. CALCULATIONS AND COMPARISONS

For comparison to known results we calculated the actions and amplitudes for the  $(k, n)$  recurrence strengths in hydrogen at  $F_o = 1985$  V/cm and  $\epsilon = -3.0$  and scaled these values into the range of the experiments and calculations. Hydrogen is the simplest case to study the scaling behavior of the spectra because there is no core to complicate the scaling recurrence strengths. Most experiments have been done on alkali-metal atoms, but the short action alkali spectrum is usually very similar to hydrogen. The differences are due to the quantum defects of the core. Courtney *et al.* at MIT have published calculations and experimental results for lithium in the field range  $1.8 < F < 11$  V/cm (low field, high  $n$ ,  $60 < n < 95$ ) with the electron excited from  $3s$  to  $np$  states [3]. The Wesleyan experiments were performed on singlet and triplet helium in the field range  $185 < F < 890$  V/cm (high field, low  $n$ ,  $20 < n < 30$ ) and the electron was excited from the  $2s$  to  $np$  states [7]. Figure 2 shows the calculated semiclassical recurrence strengths and the quantum recurrence strengths for hydrogen,  $m=0$ ,  $s$  to  $p$  excitation, at

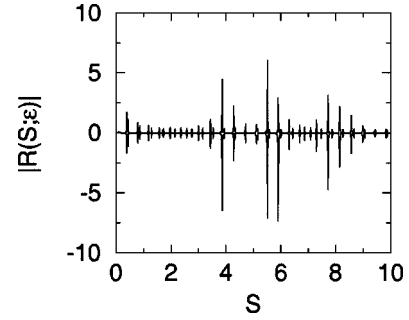


FIG. 2. Quantum (top) and primitive semiclassical (bottom)  $m=0$  recurrence spectra at  $\epsilon = -3.0$  for  $1.85 < F < 10.9$  V/cm ( $60 < n < 95$ ). The quantum spectrum is in reasonable agreement with the primitive semiclassical spectrum.

low-field strengths. Note that we plot the absolute value of the Fourier transform instead of the square of the transform to emphasize the weak features in the spectrum. The agreement is good, although the semiclassical approximation overestimates the peaks near  $\hat{S} = 5.9$  and  $7.9$ . The level of agreement is comparable to that in Ref. [6]. Figure 3 shows the calculated semiclassical recurrence strengths and the quantum recurrence strengths for hydrogen,  $m=0$ , at high-field strengths. The semiclassical recurrence strengths have increased according to the scaling law, but the general features, relatively small peaks below  $\hat{S} = 3.9$  and then the first large peak at  $\hat{S} = 3.9$ , etc., have not changed.

A comparison to the quantum spectrum [25–27], however, shows significant changes between the low-field and the high-field recurrence spectra. In the quantum calculation, the large peaks near  $\hat{S} = 3.9$  and  $5.9$  seen at lower-field strengths are greatly suppressed relatively to the recurrence strengths of the other orbits at higher-field strengths. There is now a cluster of peaks of essentially the same heights in the range  $3.8 < \hat{S} < 6$ . In Fig. 4 we show the semiclassical and the quantum  $m=1$  spectrum at high fields. These are, in contrast to the  $m=0$  results, in good agreement. The  $m=1$  semiclassical recurrence spectrum was calculated using the  $m=0$  orbits and changing the angular distribution of the outgoing waves [28]; therefore, the closed orbits in Fig. 4 are the same

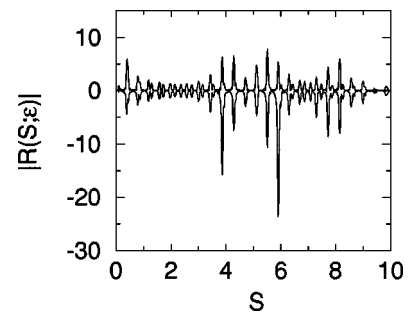


FIG. 3. Quantum (top) and semiclassical (bottom)  $m=0$  recurrence spectra at  $\epsilon = -3.0$  for  $176 < F < 890$  V/cm. The quantum spectrum does not agree with the primitive semiclassical spectrum. In particular, the pattern of large peaks in the range  $3.9 < \hat{S} < 6$  is completely different. The large peaks just below  $\hat{S} = 4, 6,$  and  $8$  are from repetitions of the uphill and the downhill orbits that are near bifurcations (see Fig. 6).

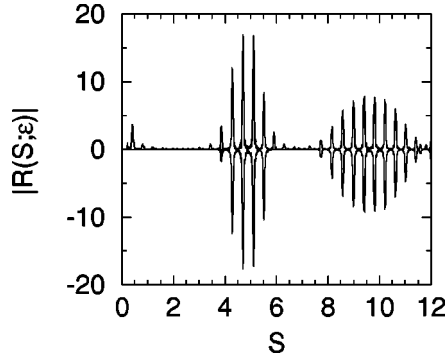


FIG. 4. Quantum (top) and semiclassical (bottom)  $m=1$  recurrence spectra at  $\epsilon = -3.0$  for  $176 < F < 890$  V/cm ( $20 < n < 30$ ). The quantum spectrum and the semiclassical spectrum show good agreement. The uphill and downhill orbits are completely absent in the semiclassical spectrum, but *ghost* peaks near the bifurcations are visible in the quantum result.

orbits used in Fig. 3. The  $m=1$  semiclassical spectrum, however, does not contain recurrences from the uphill and downhill orbits since they lie in the nodes of the angular distribution produced by the laser. The slightly high recurrence strengths in the low field  $m=0$  spectrum are also a clue. They are associated with the 15th return of the uphill orbit and 9th and 18th returns of the downhill orbits and these are near bifurcations. From the discussion of Eqs. (22) and (23), we expect deviations from the classical scaling near the bifurcations.

We calculated the uniform recurrence amplitudes and compared them to the primitive recurrence amplitudes in the two different field strength ranges. The recurrence strength after Fourier transformation is proportional to the recurrence amplitude of the orbit [13,29]. Figure 5 shows the calculated recurrence amplitudes as a function of  $\epsilon$  for the 15th return of the uphill orbit, the return responsible for the peak at  $\hat{S} = 5.9$ . Both the uniform and the primitive results are shown: one at the average field strength of the MIT experiments and the other at the average field strength of the Wesleyan experiments. At either end of the scaled-energy range plotted, the uniform and primitive are starting to agree. However, the width of the region where they disagree increases as the field strength increases.

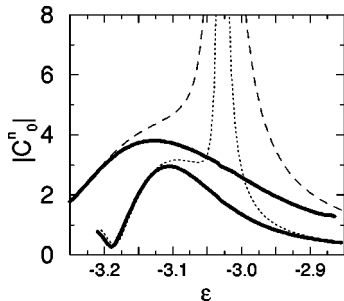


FIG. 5. Recurrence amplitude for the  $n=15$  recurrence of the uphill orbit is shown for a range of scaled energies near  $\epsilon = -3.0$  at the field strengths  $F=5$  V/cm (lower solid line) and  $F=534$  V/cm (upper solid line). The dashed and the dotted lines are the respective primitive recurrence amplitudes. The bifurcation occurs near  $\epsilon = -3.028$ . This recurrence is the peak near  $\hat{S}=5.9$  in Fig. 3.

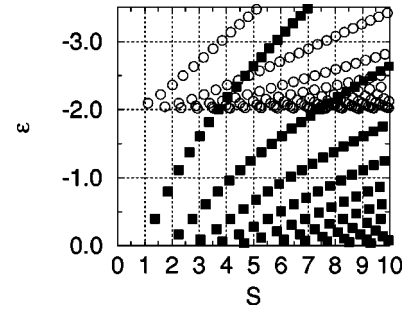


FIG. 6. Locations of bifurcations of the uphill and downhill orbits plotted vs the scaled energy. The circles are the bifurcation energies of the downhill orbit and the squares are the bifurcation locations of the uphill orbit. Notice the accumulation of bifurcations just below  $\epsilon = -2$  and 0.

At low fields and high  $n$ ,  $n \approx 80$ , the primitive semiclassical approximation is reasonably close to the uniform result at  $\epsilon = -3.0$ , but it is already starting to diverge. The bifurcation energy is  $\epsilon = -3.02877$  and  $\epsilon = -3.0$  is on the forbidden side of the bifurcation where complex orbits affect the recurrence strength. At high fields and low  $n$ ,  $n \approx 25$ , the primitive semiclassical result has increased by  $(F/F_0)^{1/4}$ , about a factor of 3, and the uniform result has increased only slightly. As the other closed-orbit recurrence strengths increased according to the scaling law, the recurrence strengths of the orbits near the  $\pm z$  axis did not increase at the predicted rate when they were near bifurcations. There the increase in the recurrence strength was much slower than the prediction. This is the main cause of the deviations from the scaling law in the recurrence spectra and explains the change from relative agreement to complete disagreement seen in Figs. 2 and 3. Since there are many bifurcations in this system, this nonscaling is typical and at any scaled energy some return of the uphill or downhill will pass close to a bifurcation. Figure 6 shows the positions of the bifurcations of the uphill and downhill orbits versus scaled action and scaled energy. The downhill orbit only exists below  $\epsilon = -2$  and many bifurcations are encountered just below this scaled energy.

The range of scaled energy about the bifurcation energy where the uniform approximation is needed can be estimated from the action inequality

$$\left| \frac{a_1^2}{4a_3} \right| \leq F^{1/4}, \quad (24)$$

which comes from Eq. (13) evaluated at the real or complex roots  $p'_v = \pm \sqrt{-a}$  and Eq. (8). This formula can be used on either side of the bifurcation. The coefficients  $a_1$  and  $a_3$  are independent of the field strength because the shape of the manifold depends only on the value of  $\epsilon$ . Thus the manifold needs only to be calculated once at each scaled energy and the inequality can be checked in the field strength range of the experiment.

Figure 7 shows the  $m=0$  quantum and the uniform semiclassical calculation. The agreement between the two is now very good. To construct the uniform semiclassical recurrence

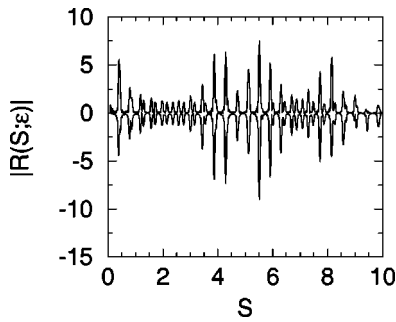


FIG. 7. Quantum (top) and uniform semiclassical (bottom)  $m=0$  recurrence spectra at  $\epsilon=-3.0$  for  $176 < F < 890$  V/cm. The agreement is now very good.

spectrum the uniform approximation also had to be applied to the 9th and 18th returns of the downhill orbit, which have a bifurcation at  $\epsilon=-3.01903$ .

If we know the uniform recurrence strength can we scale that result to get the uniform recurrence strength at another field strength at fixed  $\epsilon$ ? The field strength dependence of the recurrence strength is in the  $\lambda$  dependence of Eqs. (22) and (23). There are only three simple cases. At the bifurcation Eq. (22) simplifies and scales like  $(F/F_0)^{1/8}$ . The finite difference term in Eq. (23) reduces the contribution from Eq. (22) and it always scales as  $(F/F_0)^{1/4}$ . Neither term dominates the other at the bifurcation, so the observed variation in the recurrence strength with field strength does not follow either scaling law though each part scales separately. Before the bifurcation, when the roots are complex, the asymptotic form of Eq. (22) is proportional to  $(F/F_0)^{1/4}$  and when combined with the finite-difference term goes over to the scaling law for the uphill or downhill orbit. Past the bifurcation, when the asymptotic form of Eq. (22) goes over to two terms that scale as  $(F/F_0)^{1/8}$  and  $(F/F_0)^{1/4}$ , we recover the scaling laws for the separated primitive recurrences. However, away from the bifurcation but before the primitive results can be used, no simple scaling law can be extracted from Eq. (22) at a fixed scaled energy. The direct calculation of the recurrence strengths as a function of  $\epsilon$  and  $F$  is straightforward though once the complex momenta are properly included.

#### IV. CONCLUSIONS

In the range  $\epsilon < -2$  where the uphill and the downhill orbits are both bifurcating, almost any choice of  $\epsilon$  will pass

near a bifurcation on some repetition of those closed orbits. As the field strength is increased, the scaled-energy range around the bifurcations where the primitive closed-orbit theory fails gets wider according to Eq. (24). This makes closed-orbit theory more difficult to apply, but the repair is straightforward for hydrogen. We have also derived a formula for the scattered wave near the bifurcation for alkali-metal atoms and this will be explored in another paper.

The change from good agreement with a primitive semiclassical calculation to poor agreement at  $\epsilon=-3$  as the field strength is varied for the  $m=0$  recurrence spectra can be understood as a variation in the effective size of  $\hbar$  and a breakdown of the isolated orbit approximation for the orbits on the  $\pm z$  axes. The isolated closed-orbit results are good for the orbits away from the axes, so the  $m=1$  recurrence spectra, where the recurrences of the on axis orbits are suppressed, do not show deviations from the scaling law. Modifications to the uniform approximation to include complex orbits allow us to accurately calculate the recurrence strength for the  $m=0$  spectra for different scaled energies and electric field strengths and study the deviations from the classical scaling law.

The uniform approximation used here replaces the isolated-closed-orbit approximation by an isolated-cusp approximation: It presumes that the on-axis and bifurcated orbits are well separated from any other closed orbits. More complicated cases also arise. For example, the  $n$ th return of the downhill orbit has  $n-1$  bifurcations that get closely spaced in scaled energy as  $\epsilon=-2$  is approached from below (Fig. 6). In these cases the isolated-orbit approximation will certainly break down, but the isolated-cusp, cubic-manifold approximation we used to calculate our uniform wave functions will also break down as the manifold coils into a spiral and multiple stationary phase points exist within  $\hbar$  of one another. Then an approach using normal forms [9,30] may be required to calculate the returning wave function entering into Eq. (1). There is still interesting work to be done before we have a complete semiclassical understanding of even the hydrogen Stark spectrum.

#### ACKNOWLEDGMENTS

J.S. thanks John Delos and Jing Gao for valuable discussions and a critical reading of the manuscript. Len Keeler and Tom Morgan have shared their experimental data. This work was supported by the NSF and the U.S. Department of Energy with Auburn University.

- 
- [1] A. Holle, J. Main, G. Weibusch, H. Rottke, and K. H. Welge, *Phys. Rev. Lett.* **61**, 161 (1988).
  - [2] T. van der Veldt, Doctoral thesis, Vrije Universiteit te Amsterdam, 1993 (unpublished); T. van der Veldt, W. Vassen, and W. Hogervorst, *Europhys. Lett.* **21**, 903 (1993).
  - [3] M. Courtney, N. Spellmeyer, H. Jiao, and D. Kleppner, *Phys. Rev. A* **51**, 3604 (1995).
  - [4] M. L. Du and J. B. Delos, *Phys. Rev. A* **38**, 1896 (1988); **38**, 1913 (1988).
  - [5] E. B. Bogomolnyi, *Sov. Phys. JETP* **69**, 275 (1989); E. B. Bogomolnyi, *JETP Lett.* **47**, 526 (1988).
  - [6] P. A. Dando, T. S. Monteiro, D. Delande, and K. T. Taylor, *Phys. Rev. A* **54**, 127 (1996); P. A. Dando, T. S. Monteiro, D. Delande, and K. T. Taylor, *Phys. Rev. Lett.* **74**, 1099 (1995).
  - [7] L. Keeler and T. Morgan (private communication); A. Kips (private communication).
  - [8] J. Main and G. Wunner, *Phys. Rev. A* **55**, 1743 (1997).
  - [9] H. Schomerus and M. Sieber, *J. Phys. A* **30**, 4537 (1997).
  - [10] J. N. L. Connor, *Mol. Phys.* **25**, 181 (1973); **26**, 1217 (1973); **26**, 1371 (1973); **31**, 33 (1976).
  - [11] J. B. Delos, *Adv. Chem. Phys.* **65**, 161 (1986); R. Littlejohn, *J. Stat. Phys.* **68**, 7 (1992).

- [12] O. de Almeida, *Hamiltonian Systems: Chaos and Quantization* (Cambridge University Press, Cambridge, 1988); V. I. Arnold, *Mathematical Methods of Classical Mechanics* (Springer-Verlag, Berlin, 1989).
- [13] J. Gao and J. B. Delos, Phys. Rev. A **46**, 1449 (1992).
- [14] K. R. Meyer, Trans. Am. Math. Soc. **149**, 95 (1970).
- [15] L. S. Schulman, *Techniques and Applications of Path Integration* (Wiley, New York, 1981).
- [16] J. Gao, Ph.D. thesis, College of William and Mary, 1994 (unpublished); M. Courtney, H. Jiao, N. Spellmeyer, D. Kleppner, J. Gao, and J. B. Delos, Phys. Rev. Lett. **74**, 1538 (1995).
- [17] J. Gao and J. B. Delos, Phys. Rev. A **56**, 356 (1997).
- [18] J.-M. Mao, J. Shaw, and J. B. Delos, J. Stat. Phys. **68**, 51 (1992).
- [19] J. Shaw, J. Delos, M. Courtney, and D. Kleppner, Phys. Rev. A **52**, 3695 (1995).
- [20] A. Peters, Charles Jaffe, J. Gao, and J. B. Delos, Phys. Rev. A **56**, 345 (1997).
- [21] V. P. Maslov and M. V. Fedoriuk, *Semi-Classical Approximation in Quantum Mechanics* (Reidel, Dordrecht, 1981).
- [22] *Handbook of Mathematical Functions*, Natl. Bur. Stand. Appl. Math. Ser. No. 55, edited by M. Abramowitz and I. Stegun (U.S. GPO, Washington, DC, 1964).
- [23] W. Press, S. Teulkolsky, W. Vetterling, and B. Flannery, *Numerical Recipes in Fortran*, 2nd ed. (Cambridge University Press, Cambridge, 1992).
- [24] N. Bleistein, Commun. Pure Appl. Math. **19**, 353 (1966).
- [25] U. Fano, Phys. Rev. A **24**, 619 (1981).
- [26] D.A. Harmin, Phys. Rev. A **24**, 2491 (1981); **26**, 2656 (1982).
- [27] F. Robicheaux and J. Shaw, Phys. Rev. A **56**, 278 (1997).
- [28] J. Goetz and J. B. Delos, in *Quantum Dynamics of Chaotic Systems*, Proceedings of the Third Drexel Symposium on Quantum Nonintegrability, Philadelphia, 1993, edited by J. Yuan, D. Feng, and G. Zaslavsky (Gordon and Breach, New York, 1993).
- [29] J. Main, G. Wiebusch, K. H. Welge, J. Shaw, and J. B. Delos, Phys. Rev. A **49**, 847 (1994).
- [30] A. M. O. de Almeida and J. H. Hannay, J. Phys. A **20**, 5873 (1987).